J. Chem. Sci., Vol. 118, No. 4, July 2006, pp. 319–326.

Substitution reactions of diphenyl-2-pyridylphosphine with $[(h^5\text{-}C_5Me_5)M(m\text{-}Cl)Cl]_2$ (M = Rh or Ir) dimers: Isolation of mono-, di- and chelating complexes

PADAVATTAN GOVINDASWAMY[a], PATRICK J CARROLL[b], YURIJ A MOZHARIVSKYJ[c] and MOHAN RAO KOLLIPARA[a,*]

[a]Department of Chemistry, North-Eastern Hill University, Shillong 793 022
[b]Department of Chemistry, University of Pennsylvania, Philadelphia, Pennsylvania PA 19104, USA
[c]Department of Chemistry, McMaster University, Hamilton, Ontario, L8S 4M1, Canada
e-mail: mohanrao59@hotmail.com; mohanraokollipara@yahoo.co.in

MS received 30 March 2006; revised 3 July 2006

Abstract. The reaction of $[\{(h^5\text{-}C_5Me_5)M(m\text{-}Cl)Cl\}_2]$ {where M = Rh (**1**), Ir (**2**)} with functionalized phosphine viz., diphenyl-2-pyridylphosphine (PPh_2Py) in dichloromethane solvent yield neutral k^1-P-coordinated rhodium and iridium complexes $[(h^5\text{-}C_5Me_5)RhCl_2(k^1\text{-}P\text{-}PPh_2Py)]$ **3** and $[(h^5\text{-}C_5Me_5)IrCl_2(k^1\text{-}P\text{-}PPh_2Py)]$ **4**. Reaction of complexes **1** and **2** with the ligand PPh_2Py in methanol under reflux give *bis*-substituted complexes such as $[(h^5\text{-}C_5Me_5)RhCl(k^1\text{-}P\text{-}PPh_2Py)_2]^+$ **5** and $[(h^5\text{-}C_5Me_5)IrCl(k^1\text{-}P\text{-}PPh_2Py)_2]^+$ **6**, whereas stirring in methanol at room temperature gives P-, N-chelating complexes of the type $[(h^5\text{-}C_5Me_5)RhCl(k^2\text{-}P\text{-}N\text{-}PPh_2Py)]^+$ **7** and $[(h^5\text{-}C_5Me_5)IrCl(k^2\text{-}P\text{-}N\text{-}PPh_2Py)]^+$ **8**. Neutral k^1-P-coordinated complexes $[(h^5\text{-}C_5Me_5)RhCl_2(k^1\text{-}P\text{-}PPh_2Py)]$ **3** and $[(h^5\text{-}C_5Me_5)IrCl_2(k^1\text{-}P\text{-}PPh_2Py)]$ **4** easily undergo conversion to the cationic P-, N-chelating complexes $[(h^5\text{-}C_5Me_5)RhCl(k^2\text{-}P\text{-}N\text{-}PPh_2Py)]^+$ **7** and $[(h^5\text{-}C_5Me_5)IrCl(k^2\text{-}P, N\text{-}PPh_2Py)]^+$ **8** on stirring in methanol at room temperature. These complexes are characterized by FT–IR and FT–NMR spectroscopy as well as analytical methods. The molecular structures of the representative complexes $[(h^5\text{-}C_5Me_5)RhCl_2(k^1\text{-}P\text{-}PPh_2Py)]$ **3**, $[(h^5\text{-}C_5Me_5)IrCl_2(k^1\text{-}P\text{-}PPh_2Py)]$ **4** and hexafluorophosphate salt of complex $[(h^5\text{-}C_5Me_5)IrCl(k^2\text{-}P\text{-}PPh_2Py)_2]^+$ **6** are established by single-crystal X-ray diffraction methods.

Keywords. Pentamethylcyclopentadienyl; diphenyl-2-pyridylphosphine; rhodium and iridium complexes.

1. Introduction

The dimeric chloro-bridged complexes $[\{(h^5\text{-}C_5Me_5)M(m\text{-}Cl)Cl\}_2]$ (M = Rh or Ir) have been the subject of investigation by many research groups as they are very useful starting materials.[1] These complexes display some rich chemistry by cleavage of the chloro-bridge, leading to the formation of a series of interesting neutral and cationic mononuclear complexes.[2] We earlier reported on the reactivity differences of *p*-cymene and hexamethylbenzene ruthenium dimers towards diphenyl(2-pyridyl)phosphine[3]; there is also one report available on the reaction of this ligand with $[CpRu(PPh_3)_2Cl]$.[4]

Phosphines are among the most important ligands in organometallic chemistry, with a wide range of steric and electronic properties. They have found widespread application in transition metal-catalysed asymmetric syntheses. The catalytic activity of these complexes ranges from hydrogen transfer[5] to ring-closing metathesis.[6] Diphenyl(2-pyridyl)phosphine (figure 1) is a versatile ligand which can coordinate to the metal in mono-dentate, chelate and bridge form, depending on the requirements at the metal centre.[7,8] Preliminary reactions of this ligand with dimers have been reported earlier.[9]

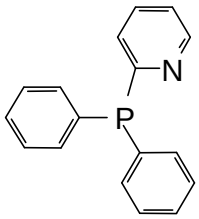

Figure 1. Structure of diphenyl(2-pyridyl)phosphine ligand.

*For correspondence

Herein, we present the syntheses of pentamethylcyclopentadienyl rhodium and iridium complexes containing PPh_2Py in neutral mono-dentate, bidentate or chelating mode.

2. Experimental

All solvents were dried and distilled before use, following standard procedures. $RhCl_3 \cdot xH_2O$ and $IrCl_3 \cdot xH_2O$ were purchased from Arora Matthey Ltd and used as such. Pentamethylcyclopentadienyl and diphenyl(2-pyridyl)phosphine were purchased from Merck and Aldrich respectively, and used as received. The precursor complexes $[\{(h^5\text{-}C_5Me_5)M(m\text{-}Cl)\}_2Cl_2]$ {where M = Rh (**1**), Ir (**2**)} were prepared according to known methods.[10] Elemental analyses were performed on a Perkin–Elmer-2400 CHN/O analyser. Infrared spectra were recorded on a Perkin–Elmer model 983 spectrophotometer with samples prepared as KBr pellets. Electronic spectra were recorded on a Hitachi-300 spectrophotometer. NMR spectra were recorded on Bruker-AMX-400 (400 MHz) and Bruker-ACF-300 (300 MHz) spectrometers with TMS as internal standard. $^{31}P\ \{^1H\}$ NMR chemical shifts are reported relative to H_3PO_4 (85%).

2.1 *Preparation of $[(h^5\text{-}C_5Me_5)MCl_2(k^1\text{-}P\text{-}PPh_2Py)]$ {M = Rh (**3**), Ir (**4**)}*

A mixture of $[\{(h^5\text{-}C_5Me_5)M(m\text{-}Cl)Cl\}_2]$ {M = Rh (**1**), Ir (**2**)}(0·162 mmol) and diphenyl-2-pyridylphosphine (PPh_2Py) (0·405 mmol) in dichloromethane (15 ml) were stirred at room temperature for 10 h. The orange solution was concentrated to 3 ml and then excess of hexane was added to precipitate it. The orange microcrystalline product separated out. The orange product was filtered and washed with diethyl ether and dried under vacuum.

*Complex **3*** – Yield 84% (155 mg). Elemental analysis for $C_{27}H_{29}RhPNCl_2$: calculated – C 56·66, H 5·10, N 2·45%; found – C 56·47, H 5·06, N 2·50%.
^1H NMR ($CDCl_3$, d): 1·39 (*d*, 15H, J_{P-H} = 3·44 Hz, C_5Me_5), 7·34–7·54 (*m*, 8H), 7·93 (*t*, 5H, J_{H-H} = 8·52 Hz), 8·69 (*d*, 1H, J_{H-H} = 6·12 Hz, *a*-proton of pyridine).
$^{31}P\ \{^1H\}$ NMR ($CDCl_3$, d): 28·75 (*d*, J_{Rh-P} = 373·6 Hz).
IR (CsI pellets, cm^{-1}): $n_{(Rh-Cl)}$ 292 (*s*). IR (KBr pellets, cm^{-1}): 1626 (*s*), 1434 (*s*), 751 (*s*), 698 (*s*), 579 (*s*).
UV-visible (CH_2Cl_2): l_{max} = 407 nm.
*Complex **4*** – Yield 87% (145 mg). Elemental analysis for $C_{27}H_{29}IrPNCl_2$: calculated C 49·01, H 4·41, N 2·12%; found – C 49·37, H 4·33, N 2·31%.
^1H NMR ($CDCl_3$, d): 1·37 (*d*, 15H, J_{P-H} = 2·16 Hz, C_5Me_5), 7·19–7·56 (*m*, 11H), 7·89 (*t*, 2H, J_{H-H} = 9·12 Hz), 8·68 (*d*, 1H, J_{H-H} = 5·67 Hz, *a*-proton of pyridine).
$^{31}P\ \{^1H\}$ NMR ($CDCl_3$, d): 26·17 (*s*).
IR (CsI pellets, cm^{-1}): $n_{(Ir-Cl)}$ 286 (*s*). IR (KBr pellets, cm^{-1}): 1633 (*s*), 1573 (*s*), 1447 (*s*), 751 (*s*), 698 (*s*), 532 (*s*).
UV-visible (CH_2Cl_2): l_{max} = 363 nm.

2.2a *Preparation of $[(h^5\text{-}C_5Me_5)MCl(k^1\text{-}P\text{-}PPh_2Py)_2]PF_6$ {M = Rh (**5**), Ir (**6**)}:*

A mixture of $[\{(h^5\text{-}C_5Me_5)M(m\text{-}Cl)Cl\}_2]$ {M = Rh (**1**), Ir (**2**)} (0·162 mmol) and diphenyl(2-pyridyl)phosphine (PPh_2Py) (0·81 mmol) and NH_4PF_6 (0·81 mmol) in methanol (20 ml) were refluxed for 4 h. The yellow solution was concentrated under reduced pressure. The yellow residue was dissolved in dichloromethane and filtered. The filtrate was concentrated to 2 ml and an excess of hexane was added for precipitation. The yellow-coloured product was filtered and washed with diethyl ether and dried under vacuum.

*Complex **5*** – Yield 85% (260 mg). Elemental analysis for $C_{44}H_{43}RhP_3N_2ClF_6$: calculated – C 56·92, H 4·58, N 2·96%; found – C 56·94, H 4·78, N 2·01%.
^1H NMR ($CDCl_3$, d): 1·67 (*d*, 15H, J_{P-H} = 4·64, C_5Me_5), 7·39–8·07 (*m*, 22H), 8·30 (*t*, 2H, J_{H-H} = 6·13 Hz), 8·56 (d, 2H, J_{H-H} = 4·56 Hz), 8·79 (*d*, 2H, J_{H-H} = 4·75 Hz, *a*-proton of pyridine).
$^{31}P\ \{^1H\}$ NMR ($CDCl_3$, d): –12·35 (*s*).
IR (CsI pellets, cm^{-1}): $n_{(Rh-Cl)}$ 248 (*s*). IR (KBr pellets, cm^{-1}): 1639 (*m*), 1580 (*m*), 1440 (*s*), 844 (*s*), 744 (*s*), 698 (*s*), 551 (*s*).
UV-visible (CH_2Cl_2): l_{max} = 394 nm.

*Complex **6*** – Yield 81% (210 mg). Elemental analysis for $C_{44}H_{43}IrP_3N_2ClF_6$: calculated – C 51·09, H 4·15, N 1·70%; found – C 51·13, H 4·19, N 1·82%.
^1H NMR ($CDCl_3$, d): 1·18 (*d*, 15H, J_{P-H} = 2·30 Hz, C_5Me_5), 7·05–7·55 (*m*, 26H), 8·45 (*d*, 2H, J_{H-H} = 5·36 Hz, *a*-proton of pyridine).
$^{31}P\ \{^1H\}$ NMR ($CDCl_3$, d): –10·57 (*s*).
IR (CsI pellets, cm^{-1}): $n_{(Ir-Cl)}$ 254 (*s*).
IR (KBr pellets, cm^{-1}): 1626 (*m*), 1447 (*s*), 844 (*s*), 751 (*s*), 704 (*s*), 565 (*s*), 525 (*s*).
UV-visible (CH_2Cl_2): l_{max} = 413 nm.

2.2b *Preparation of [(h^5-C_5Me_5)MCl(k^2-P-N-PPh_2Py)] PF_6 {M = Rh (**7**), Ir (**8**)} – Method 1*: A mixture of [{(h^5-C_5Me_5)M(m-Cl)Cl}$_2$] {M = Rh (**1**), Ir (**2**)} (0·162 mmol), diphenyl(2-pyridyl)phosphine (PPh_2Py) (0·324 mmol) and NH_4PF_6 (0·405 mmol) in methanol (20 ml) was stirred at room temperature for 2 h. The yellow solution was concentrated under reduced pressure. The yellow residue was dissolved in dichloromethane and filtered. The filtrate was concentrated to 2 ml and an excess of hexane was added for precipitation. The yellow-coloured product was filtered and washed with diethyl ether and dried under vacuum.

Method 2: A mixture of the complex [(h^5-C_5Me_5)MCl_2(k^1-P-PPh_2Py)] {M = Rh (**3**), Ir (**4**)} (0·162 mmol) and NH_4PF_6 (0·486 mmol) in methanol (15 ml) was stirred at room temperature for 4 h. The clear orange yellow solution was then rotary evaporated. The residue was extracted with dichloromethane and filtered to remove insoluble material. The filtrate was then reduced to about 2 ml and addition of excess hexane gave yellow solid.

*Complex **7*** – Yield 82% (180 mg). Elemental analysis for $C_{27}H_{29}RhClNP_2F_6$: calculated – C 47·56, H 4·28, N 2·05%; found – C 47·23, H 4·56, N 2·17%.
^{1}H NMR ($CDCl_3$, d): 1·68 (*d*, 15H, $J_{P–H}$ = 4·68 Hz, C_5Me_5), 7·55–7·61 (*m*, 8H), 7·83–8·07 (*m*, 5H), 8·55 (*d*, 1H, $J_{H–H}$ = 4·96 Hz), *a*-proton of pyridine).
^{31}P {^{1}H} NMR ($CDCl_3$, d): –12·49 (*d*, $J_{Rh–P}$ = 288 Hz).
IR (CsI pellets, cm^{-1}): $n_{(Rh–Cl)}$ 258 (*s*).
IR (KBr pellets, cm^{-1}): 1626 (*s*), 1440 (*s*), 1394 (*m*), 1102 (*m*), 844 (*s*), 758 (*s*), 698 (*s*), 565 (*s*).
UV-visible (CH_2Cl_2): l_{max} = 379 nm.

*Complex **8*** – Yield 85% (165 mg). Elemental analysis for $C_{27}H_{29}IrClNP_2F_6$: calculated – C 42·05, H 3·79, N 1·82%; found – C 39·73, H 3·82, N 1·86%.
^{1}H NMR ($CDCl_3$, d): 1·69 (*d*, 15H, $J_{P–H}$ = 3·08 Hz, C_5Me_5), 7·46–7·66 (*m*, 8H), 7·85–8·13 (*m*, 5H), 8·52 (*d*, 1H, $J_{H–H}$ = 5·32 Hz, *a*-proton of pyridine).
^{31}P {^{1}H} NMR ($CDCl_3$, d): –32·10 (*s*).
IR (CsI pellets, cm^{-1}): $n_{(Ir–Cl)}$ 272 (*s*).
IR (KBr pellets, cm^{-1}): 1626 (*s*), 1447 (*s*), 1387 (*m*), 1096 (*m*), 844 (*s*), 744 (*s*), 698 (*s*), 559 (*s*).
UV-visible (CH_2Cl_2): l_{max} = 364 nm.

3. Structure analysis and refinement

Single crystals of compounds **3** and **4** suitable for X-ray analyses were grown by slow diffusion of hexane into dichloromethane solutions of the respective complexes**.** Single crystals of compound **6** [PF_6] were formed by slow diffusion of diethyl ether into chloroform solution. X-ray intensity data were collected on a Rigaku Mercury CCD area detector employing graphite-monochromated MoKa radiation (l = 0·71069 Å) at a temperature of 143 K. The intensity data were corrected for Lorentz and polarization effects; absorption correction was carried using the REQAB program.[11]

The structure was solved by direct methods (SIR97).[12] Refinement was performed by a full-matrix least squares method based on F^2 using SHELXL-97.[13] The weighting scheme used was $W = 1/[s^2(F_0^2) + 0{\cdot}0094P^2 + 0{\cdot}0000P]$ for complex **3** and $W = 1/[s^2(F_0^2) + 0{\cdot}0000P^2 + 0{\cdot}00007P]$ for complex **4**, where $P = (F_0^2 + 2F_c^2)/3$. Non-hydrogen atoms were refined anisotropically, while hydrogen atoms were refined using a "riding" model. Refinement converged at final values of R = 0·0206, 0·0251, 0·0431 for the compounds **3**, **4** and **6** [PF_6] respectively (for observed data F), and at values of wR_2 = 0·0351, 0·0451, 0·1039 for complexes **3**, **4** and **6** respectively (for unique reflections).

Table 1 lists the lattice constants, data collection and refinement parameters. Figures 2, 3, and 4 are ORTEP[14] representations of thermal ellipsoids of complexes **3** and **4**, displayed with 30% probability, and of the hexafluorophosphate salt of complex **6**, shown with 50% probability. Tables 2, 3 and 4 give selected bond lengths and angles for complexes **3**, **4** and **6** respectively.

4. Results and discussion

Reaction of [{(h^5-C_5Me_5)M(m-Cl)Cl}$_2$] {M = Rh (**1**), Ir (**2**)} with diphenyl(2-pyridyl)phosphine in dichloromethane yields neutral P-coordinated complexes **3** and **4**. The same reaction in methanol under refluxing conditions yields the *bis*-P-coordinated complexes [(h^5-C_5Me_5)M(k^1-P-PPh_2Py)$_2$Cl]$^+$, M = Rh (**5**) and Ir (**6**), which were isolated as hexafluorophosphate salts (scheme 1). In methanol under stirring conditions the P-, N-chelated cationic complexes [(h^5-C_5Me_5)M(κ^2-P-N-PPh_2Py)Cl]$^+$, M = Rh (**7**) and Ir (**8**) are isolated as hexafluorophosphate salts. Complexes **3** and **4** with excess of NH_4PF_6 in methanol under stirring condition yield the compounds **7** [PF_6] and **8** [PF_6] (scheme 1) respectively. These complexes are stable in air and soluble in polar solvents such as chloroform and dichloromethane,

Table 1. Crystal data and structure refinement details for complexes **3**, **4**, and **6** $[PF_6]$. $0{\cdot}5CH_2Cl_2$.

CCDC	**270852 (3)**	**270853 (4)**	**270854 (6)**
Formula	$C_{27}H_{29}NPCl_2Rh$	$C_{27}H_{29}NPCl_2Ir$	$C_{44}H_{43}ClF_6IrN_2P_3.0{\cdot}5CH_2Cl_2$
M_r	572·29	661·58	1076·83
T (K)	143(1)	143(1)	293(2)
Wavelength (Å)	0·71069	0·71069	0·71073
Crystal system	Orthorhombic	Orthorhombic	Triclinic
Space group	*Pna2₁*	*Pna2₁*	*P1*
a (Å)	31·521(2)	31·511(2)	10·0851(8)
b (Å)	8·8700(5)	8·9019(5)	10·9150(8)
c (Å)	17·8014(10)	17·8297(11)	23·7481(18)
a (°)	90	90	77·030(1)
b (°)	90	90	78·269(1)
g (°)	90	90	64·778(1)
V (Å^3)	4977·1(5)	5001·4(5)	2287·3(3)
Z	8	8	1
Crystal size (mm^3)	0·32 × 0·22 × 0·20	0·25 × 0·15 × 0·10	0·10 × 0·12 × 0·30
D_{calc} (g cm^{-3})	1·528	1·757	1·563
F(000)	2336	2592	1070
q (°)	2·57 to 27·48	2·56 to 27·48	1·77 to 28·27
Reflections collected	21513	22872	18936
Independent reflections	9805 [R(int) = 0·0186]	8810 [R(int) = 0·0361]	17294 [R(int) = 0·0160]
Completeness to q	27·48–98·6%	27·48–98·6%	28·27–89·1%
m(Mo–Ka) (mm^{-1})	9·81	5·633	3·198
Data/parameters	9805/1/588	8810/1/588	17294/5/843
Goodness-of-fit on F^2	0·880	0·876	1·059
$R1$ ($I > 2s$ (I)), $wR2$	0·0206, 0·0351	0·0251, 0·0451	0·0431, 0·1039
$R1$, $R2$ (all data)	0·0238, 0·0359	0·0281, 0·0471	0·0541, 0·1098
Largest diff. peak and hole(e.Å^{-3})	+0·523 & –0·506	+1·341 & –1·052	1·491 & –0·471

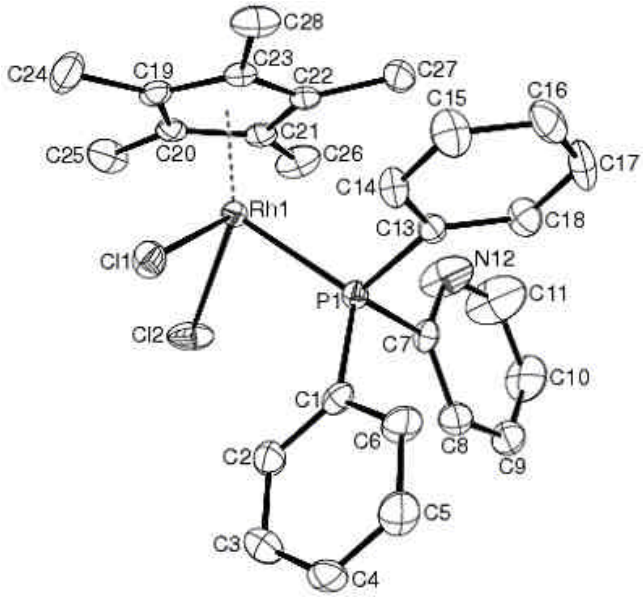

Figure 2. ORTEP diagram of complex **3** with 30% probability thermal ellipsoids. Hydrogens are omitted for clarity.

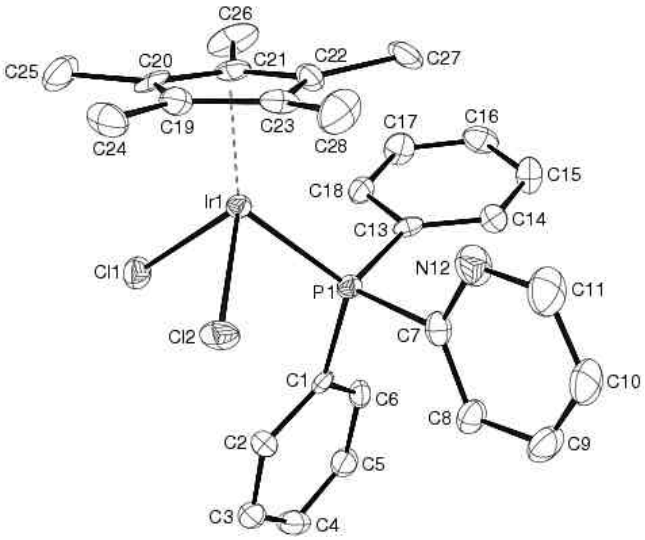

Figure 3. ORTEP diagram of complex **4** with 30% probability thermal ellipsoids. Hydrogens are omitted for clarity.

but insoluble in non-polar solvents such as hexane and pentane.

4.1 *Mono-dentate neutral complexes **3** and **4***

Spectroscopic data suggest coordination of the ligand to the metal in mono-dentate fashion as evident from

Table 2. Selected bond lengths (Å) and bond angles (°) for complex **3**.

Bond lengths					
Rh(1)–P(1)	2·3165(7)	Rh(1)–Cl(1)	2·4107(7)	Rh(1)–Cl(2)	2·4005(6)
Rh(1′)–P(1′)	2·3171(7)	Rh(1′)–Cl(1′)	2·3904(7)	Rh(1′)–Cl(2′)	2·4030(6)
Rh(1)–C*	1·8174(2)	Rh(1′)–C*	1·8236(2)		
Bond angles					
P(1)–Rh(1)–Cl(1)	88·43(2)	P(1)–Rh(1)–Cl(2)	89·03(2)		
Cl(1)–Rh(1)–Cl(2)	93·34(2)	P(1′)-Rh(1′)–Cl(1′)	89·54(2)		
P(1′)–Rh(1′)–Cl(2′)	86·59(2)	Cl(1′)-Rh(1′)–Cl(2′)	93·04(2)		

Rhodium to centroid of Cp

Table 3. Selected bond lengths (Å) and bond angles (°) for complex **4**.

Bond lengths					
Ir(1)–P(1)	2·299(2)	Ir(1)–Cl(1)	2·3990(14)	Ir(1)–Cl(2)	2·4076(13)
Ir(1′)–P(1′)	2·299(2)	Ir(1′)–Cl(2′)	2·4056(14)	Ir(1′)–C*	1·8246(2)
Ir(1)–C*	1·8297(2)	Ir(1′)–Cl(1′)	2·411(2)		
Bond angles					
P(1)–Ir(1)–Cl(1)	90·08(5)	P(1)–Ir(1)–Cl(2)	86·86(5)		
Cl(1)–Ir(1)–Cl(2)	90·21(5)	P(1′)–Ir(1′)–Cl(1′)	88·61(5)		
P(1′)–Ir(1′)–Cl(2′)	89·53(5)	Cl(1′)–r(1′)–Cl(2′)	90·65(6)		

Iridium to centroid of Cp

Table 4. Selected bond lengths (Å) and bond angles (°) for complex **6**.

Bond lengths					
Ir(A)–P(1A)	2·316(3)	Ir(A)–P(2A)	2·347(3)	Ir(A)–Cl(A)	2·387(3)
Ir(A)–C*	1·957	Ir(B)–C*	1·864		
Bond angles					
P(1A)–Ir(A)–Cl(A)	93·21(12)	P(2A)–Ir(A)–Cl(A)	89·45(12)		
P(1A)–Ir(A)–P(2A)	95·27(11)	P(1B)–Ir(B)–Cl(B)	91·76(12)		
P(2B)–Ir(B)–Cl(B)	91·49(12)	P(1B)–Ir(B)–P(2B)	95·16(13)		

Iridium to centroid of Cp

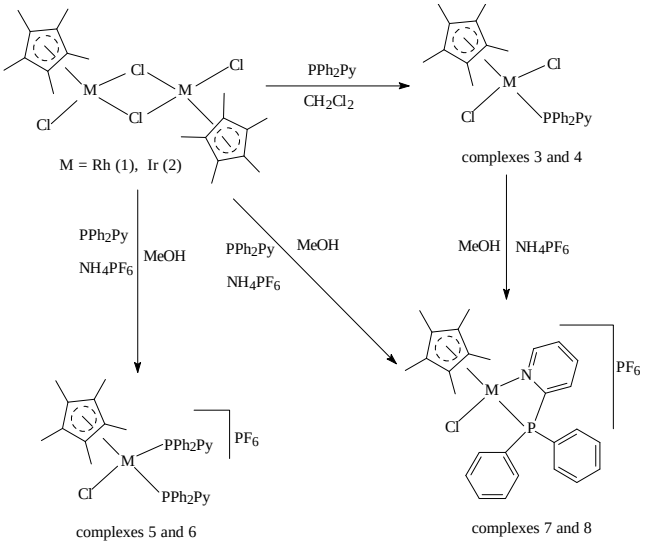

Scheme 1. Synthetic pathways.

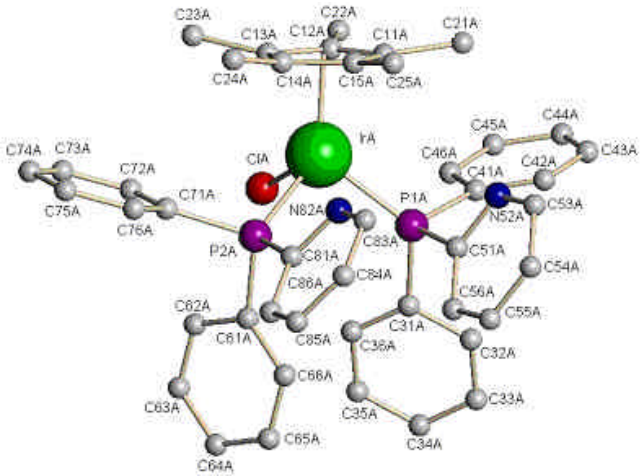

Figure 4. ORTEP diagram of complex **6** with 50% probability thermal ellipsoids. Hydrogens are omitted for clarity.

the presence of proton peaks of the ligand and shift of Cp* resonance in the proton NMR spectra compared to the starting complexes **1** and **2**. The ^{1}H NMR spectra of complexes **3** and **4** show doublets at 1·39 and 1·37 ppm for the methyl protons of the pentamethylcyclopentadienyl group, which arise from the coupling of the pentamethylcyclopentadienyl group protons with the phosphine ligand ($J_{P–H}$ = 3·44 Hz for complex **3** and $J_{P–H}$ = 2·16 Hz for complex **4**).[9] Multiplets in the aromatic region at 7·19–7·93 ppm for the phosphine ligand are also observed. The doublet at 8·69 ppm ($J_{H–H}$ = 6·12 Hz) for complex **3** and at 8·68 ppm ($J_{H–H}$ = 5·67 Hz) for complex **4** arises from the *a*-proton of the pyridine group of the PPh_2Py ligand. The ^{31}P {^{1}H} NMR spectrum of complex **3** shows one doublet at 28·75 ppm for the phosphine ligand, due to rhodium–phosphorous coupling ($J_{Rh–P}$ = 373·6 Hz), and a singlet at 26·17 ppm for complex **4**. The PPh_2Py ligand exhibits a significant downfield shift after coordination to the metal as compared to the free ligand. The far-IR spectrum shows a strong band at 286–292 cm^{-1} for the M–Cl stretching vibration mode.

4.2 *Bi-substituted cationic complexes **5** and **6***

These complexes are isolated as yellow solids and are fully characterized by elemental, infrared and NMR spectra. ^{1}H NMR spectra of complexes **5** and **6**, exhibit resonances corresponding to pentamethylcyclopentadienyl protons, observed as doublets at 1·67 ppm ($J_{P–H}$ = 4·64 Hz) and at 1·18 ppm ($J_{P–H}$ = 2·30 Hz), both arising due to Cp* protons coupling with the phosphine of the PPh_2Py ligand. It is interesting to observe that the chemical shift of the Cp* group moves downfield in the case of the rhodium complex and upfield in the iridium complex. The doublets observed at 8·79 ppm ($J_{H–H}$ = 4·75 Hz) for complex **5** and 8·45 ppm ($J_{H–H}$ = 5·36 Hz) for complex **6** in the proton NMR spectra are assigned to the *a*-proton of the pyridine ring in the PPh_2Py ligand. The phenyl group of the phosphine ligand exhibits multiplets in the range of 7·05–8·56 ppm. ^{31}P {^{1}H} NMR spectra of complexes **5** and **6** show singlets at –12·35 ppm and –10·57 ppm. It is interesting to note that in these complexes the ^{31}P nuclei of PPh_2Py exhibits an upfield shift as compared to the free ligand and neutral compounds (**3** and **4**). It is difficult to rationalize the upfield shift, which may be due to the high electron density on the metal centre arising from the two PPh_2Py ligands. Owing to the high electron density on the metal centre, one can expect that the degree of back-bonding increases from metal to ligand (*dp–pp*) in comparison with the other compounds. Presence of a single peak for two PPh_2Py indicates that the both phosphines are in the same environment.

4.3 *Chelating complexes **7** and **8***

The ^{1}H NMR spectra of complexes **7** and **8** show patterns of signals different from that of complexes **3** and **4**. The *a*-proton of the pyridine appears as a doublet at 8·55 ppm ($J_{H–H}$ = 4·96 Hz) for complex **7** and at 8·52 ppm ($J_{H–H}$ = 5·32 Hz) for complex **8**. The phenyl group protons appear as multiplets in the aromatic region at 7·46–8·13 ppm. The pentamethylcyclopentadienyl group exhibits doublets at 1·68 ppm (complex **7**) and 1·69 ppm (complex **8**) respectively. The doublets arise due to coupling between the Cp* protons and the phosphorus of the PPh_2Py ligand. The ^{31}P {^{1}H} NMR spectrum of complex **7** exhibits a doublet at –12·49 ppm ($J_{Rh–P}$ = 288 Hz) due to coupling between the phosphorus of the PPh_2Py ligand and the rhodium metal centre. Complex **8** exhibits a singlet at –32·10 ppm for chelated PPh_2Py. In the case of complex **8**, the ^{31}P NMR shift moves upfield as compared to the other complexes and there is also significant difference between the rhodium and iridium complexes in the shift positions as compared to other complexes in this series. The far-infrared spectrum shows bands at 258 and 272 cm^{-1}, which are assigned to the terminal stretching vibration mode $n_{M–Cl}$ of compounds **7** and **8**. In addition, the strong band observed at 844 cm^{-1} is due to the $n_{P–F}$ mode of the PF_6^- group.

5. Molecular structures

In order to confirm the structures suggested by the spectroscopic data, molecular structures of complexes **3** and **4**, and the hexafluorophosphate salt of complex **6** were determined by using single-crystal X-ray diffraction studies. The summary of the single-crystal X-ray structure analysis is shown in table 1. ORTEP drawings of compounds **3**, **4** and **6** [PF_6] are shown in figures 2, 3, and 4 respectively. All the compounds have two independent molecules in the unit cell.

The structures of complexes **3** and **4** consist of rhodium and iridium atoms h^5-coordinated to a pentamethylcyclopentadienyl molecule, two chloride atoms and one diphenyl(2-pyridyl)phosphine ligand (through the P atom) leading to the usual ‘three-

legged piano stool' structure. Complexes [(h^5-C_5Me_5)$RhCl_2$(k^1-P-PPh_2Py)] **3** and [(h^5-C_5Me_5)$IrCl_2$(k^1-P-PPh_2Py)] **4** crystallise in the orthorhombic space group *Pna2₁* (table 1). The geometry around the metal atom in compounds **3** and **4** may be regarded as octahedral considering that the pentamethylcyclopentadienyl group occupies three coordination positions. The M–Cl(1) and M–Cl(2) bond distances are indistinguishable (~2·4 Å), are close to reported values[15] and also similar to the M–Cl bond distances in the second molecule. M–P bond distances of 2·3165(7) and 2·299(2) Å are consistent with the distances of the cyclopentadienyl analogue of the rhodium phosphine complex (2·3089(8) Å)[9]. The centroid distance of the ring to the metal is 1·8174(2) Å for complex **3** and 1·8297(2) Å for complex **4**. The bond angles in complex **4**, namely, P(1)–Ir(1)–Cl(1), P(1)–Ir(1)–Cl(2) and Cl(1)–Ir(1)–Cl(2), are 90·08(5)°, 86·86(5)° and 90·21(5)° respectively, one similar to those in complex **3** and are characteristic of piano-stool type structures.

The hexafluorophosphate salt of complex **6** adopts a three-legged piano-stool structure with the chloride and two phosphorus atoms as the legs and with the *p*-bonded pentamethylcyclopentadienyl moiety occupying three facial coordination sites. The centroid distance in molecule A between the iridium atom and pentamethylcyclopentadienyl is 1·957 Å, which is longer than that in the molecule B (1·864 Å). There is no significant difference in the C–C bond lengths in the pentamethylcyclopentadienyl ring, all being 1·42 Å and pointing to a *p*-electron delocalization in the ring. Further, the five-membered ring is planar, as evident from the nearly equal bond distances between the metal atom and the ring carbons. The iridium–chlorine bond length (2·387(3) Å) is within the range reported for half-sandwich pentamethylcyclopentadienyl iridium complexes[16] containing an iridium-chlorine bond. The Ir–P1A and Ir–P2A bond lengths are 2·316(3) Å and 2·347(3), which are similar to those in molecule B. The bond angles P1A–IrA–ClA (93·21°), P2A-IrA–ClA (89·45°), P1A–IrA–P2A (95·27°) confirm the piano-stool structure of the complex.

6. Concluding remarks

We have synthesized new h^5-pentamethylcyclopentadienyl rhodium(III) and iridium(III) complexes containing diphenyl(2-pyridyl)phosphine ligand. Under refluxing conditions, pentamethylcyclopentadienyl rhodium and iridium dimers with PPh_2Py ligand yield the di-substituted *bis*-phosphine complexes, which may be due to the high electron density and larger size of the metal atom. This high electron density on the metal is perhaps the result of charge donation by the h^5-C_5Me_5 moiety.

Supplementary material

Crystallographic data (excluding structure factors) for the structures reported in this paper have been deposited with the Cambridge Crystallographic Data Centre as supplementary publications: No. CCDC **270852** for complex **3**, **270853** for complex **4** and **270854** for complex **6**. The data can be obtained free of charge on application to CCDC, 12 Union Road, Cambridge CB2 1EZ, UK (Fax: +(44)-1223/336033; e-mail: deposit@ccdc.cam.ac.uk or www: http://www.ccdc.cam.ac.uk).

References

1. (a) Maitlis P M 1995 *J. Organomet. Chem.* **500** 239; (b) Abel E W, Stone F G A and Wilkinson G (eds) 1982–1994 *Comprehensive organometallic chemistry II: A review of the literature* **8** 177
2. (a) Joubran C, Grotjahn D B and Hubbard J L 1996 *Organometallics* **15** 1230; (b) Carmona, E, Cingolani A, Marchetti F, Pettinari C, Pettinari R, Skelton B W and White A H 2003 *Organometallics* **22** 2820; (c) Steinke T, Gemel C, Cokoja M, Winter M and Fischer R A 2003 *Chem. Commun*. **9** 1066; (d) Ara I, Berenguer J R, Eguizabal E, Fornie J, Lalinde E and Martin A 2001 *Eur. J. Inorg. Chem*. **6** 1631
3. Govindaswamy P, Mozharivskyj Y A and Kollipara M R 2004 *Polyhedron* **23** 3115
4. Rida M A, Coperet C and Smith A K 2001 *J. Organomet. Chem*. **628** 1
5. Hauser C S, Slugove C, Mereiter K, Schimid R, Kirchner K, Xiao L and Weissenteiner W 2001 *J. Chem. Soc., Dalton Trans*. 2989
6. (a) Frstner A, Picquet M, Bruneau C and Dixneuf P H 1998 *Chem. Commun*. 1315; (b) Soderberg B C G 2003 *Coord. Chem. Rev*. **241** 147
7. (a) Alcock N W, Moore P, Lampe P A and Mock K F 1982 *J. Chem. Soc., Dalton Trans*. 207; (b) Olmstead M M, Maisonnat A, Farr J P and Balch A L 1981 *Inorg. Chem*. **20** 4060; (c) Inoguchi Y, Milewski-Marla B and Schmidbauer H 1982 *Chem. Berichte* **115** 3085; (d) Wasserman H J, Moody D C, Paine R T, Ryan R R and Salazar K V 1984 *J. Chem. Soc., Chem. Commun*. 533
8. (a) Hong F E, Chang Y C, Chang R E, Lin C C, Wang S L and Liao F L 1999 *J. Organomet. Chem*. **588** 160; (b) Wood F E, Olmstead M M, Farr J P and Balch A L 1985 *Inorg. Chim. Acta* **97** 77; (c) Abram U, Alberto R, Dilworth J R, Zheng Y and Ortner K 1999 *Polyhedron* **18** 2995

9. Drommi D, Arena C, Nicolo F, Bruno G and Faraone F 1995 *J. Organomet. Chem*. **485** 115
10. (a) Booth B L, Haszeldine R N and Hill M 1969 *J. Chem. Soc*. **A1299**; (b) White C, Yates A and Maitlis P M 1992 *Inorg. Synth*. **29** 228
11. Jacobson R A 1994 REQAB4 (a software program to calculate absorption correction) (private communication)
12. Altomare A, Burla M, Camalli M, Cascarano G, Giacovazzo C, Guagliardi A, Moliterni A, Polidori G and Spagna R J 1999 *Appl. Cryst*. **32** 115
13. Sheldrick G M 1997 SHELXL-97: Program for the refinement of crystal structures, University of Göttingen, Germany
14. Johnson C K 1976 ORTEP-II: A Fortran thermal ellipsoid plot program for crystal structure illustrations ORNL-5138
15. Aneetha H, Zacharias P S, Srinivas B, Lee G H and Wang Y 1999 *Polyhedron* **18** 299
16. Govindaswamy P and Mozharivskyj Y A and Kollipara M R 2005 *Polyhedron* **24** 1710